Analysing flow structures around a blade using spectral/hp method and HPIV

Bernhard Stoevesandt[1], Christian Steigerwald[1], Andrei Shishkin[2], Claus Wagner[2] and Joachim Peinke[1]

[1] ForWind, Marie-Curie-Str. 2 26129 Oldenburg bernhard.stoevesandt@forwind.de
[2] DLR Göttingen, Robert-Bunsenstr. 10 D-37073 Göttingen

E-mail: `bernhard.stoevesandt@forwind.de`

Abstract. A still difficult, yet pressing task for blade manufacturers and turbine producers is the correct prediction of the effects of turbulent winds on the blade. Reynolds Averaged Numerical Simulations (RANS) are a limited tool for calculating the effects. For large eddy simulations (LES) boundary layer calculation are still difficult therefore the spectral element method seems to be an approach to improve numerical calculations of flow separation.
The flow field around an fx79-w151a airfoil has been calculated by the spectral element code $\mathcal{N}\varepsilon\kappa\mathcal{T}\alpha r$ using a direct numerical simulation (DNS) solver. In a first step a laminar inflow on the airfoil at angle of attack of $\alpha = 12^0$ and a Reynolds number of $Re = 33000$ was simulated using the 2D Version of the code. The flow pattern was compared to measurements using holographic particle induced velocimetry (HPIV) in a wind tunnel.

1. Introduction

A still difficult, yet pressing task for blade manufacturers and turbine producers is the correct prediction of the effects of turbulent winds on the blade. As in turbulent wind the blade is expected to be frequently submitted to the dynamic stall effect[1], precise calculations of the flow around the blade which are time resolved are of high interest[2].

Since the RANS methods are limited in precision in respect to time resolved turbulence simulations[3], LES and detached eddy simulations (DES) have become more attractive in recent years as computational power increased. For the flow around airfoils the European LESFOIL project was an essential step forward in practical using of LES as alternative to RANS modelling. The the flow around an Aerospatiale-A airfoil at the Reynolds number of $Re = 2.1 \cdot 10^6$ and an angle of attack $\alpha = 13.3^0$ was investigated[4]. The results revealed the strengths of the LES model but also the difficulties especially considering the resolution and the near-wall modelling at the leading- and trailing edge.

While the simulation at high Reynolds numbers has been difficult, some groups have turned to simulate the flow for lower Reynolds numbers to start off with [5][6][7]. Nevertheless the boundary layer resolution remains a difficult task. Therefore hybrid RANS/LES methods and DES have been applied to overcome the problems[8][9]. Yet in these models there is still numerical dissipation applied, which might lead to some deviances.

The spectral element method seems to be a different, promising method to overcome the resolution problems. It combines the flexibility of finite element methods with the accuracy
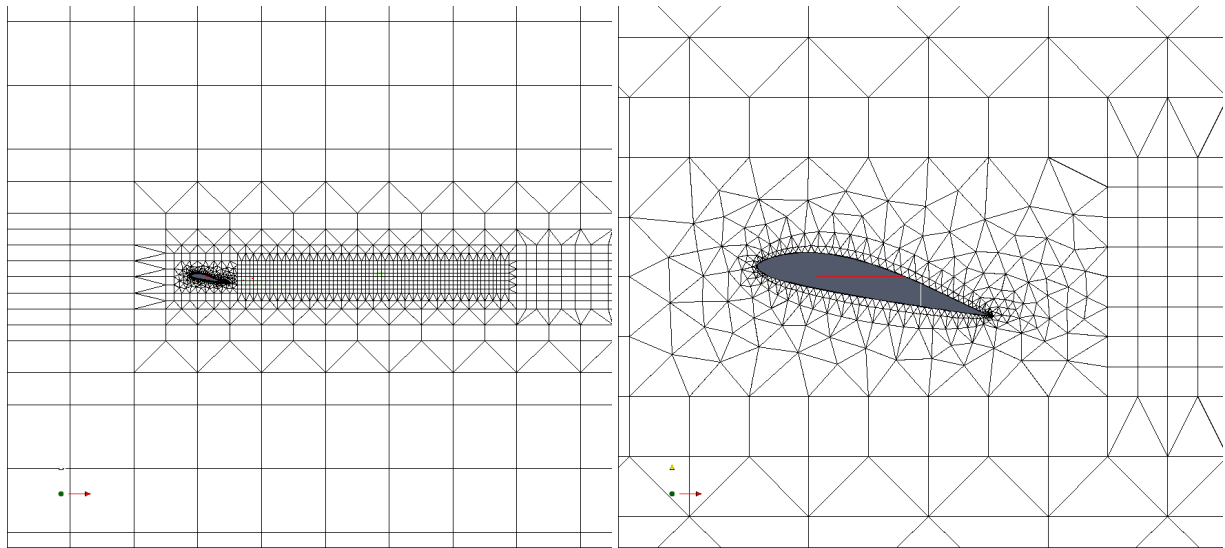
Figure 1: The grid of the domain showing a layer of fine quadrilaterals in the wake (left). The connection between the geometry of the airfoil and the rectangular mesh in most of the domain is done by using triangles (right).

of spectral methods for simulations[10] as the accuracy increases exponentially with the polynomial order. The value of the method has been verified on some applications like cylinder flows[12][13][14].
In this study the possibility to apply the method for the simulation of the flow around an airfoil for wind turbines at low Reynolds numbers is supposed to be evaluated. The results are being compared to holographic PIV measurements, a rather new method to measure 3D flows.

2. Simulation conditions

The simulation was done running the spectral element code $\mathcal{N}\varepsilon\kappa\mathcal{T}\alpha r$ using a direct numerical simulation (DNS) solver. The flow around a fx79w-151a airfoil at an angle of attack of $\alpha = 12°$ and a Reynolds number of Re=33000 based on the free stream velocity u_∞ and the chord length L_c, $Re = \frac{u_\infty L_c}{\nu}$, has been investigated. As the Reynolds number is quite high for DNS, in this study as first step the 2D solver has been used to test the general flow pattern and the stability of the simulation. A hybrid mesh using quadrilaterals around the airfoil, in the periphery and wake was used. The connection between the quadrilateral layers is being done by triangular elements. Over all 2116 elements are used (fig.1). The solver uses the incompressible Navier-Stokes equation:

$$\nabla \cdot \mathbf{u} = 0, \frac{\partial \mathbf{u}}{\partial t} + (\mathbf{u} \cdot \nabla)\mathbf{u} = -\nabla p + \nu\Delta\mathbf{u} + \mathbf{F} \tag{1}$$

These equations can be rewritten shortly as

$$\frac{\partial \mathbf{u}}{\partial t} + N(\mathbf{u}) = -\nabla p + L(\mathbf{u}), \tag{2}$$

The spectral/hp element approach developed by Karniadakis&Sherwin [10] and co-workers uses the high order splitting scheme for Navier-Stokes equations proposed by Karniadakis, Israeli & Orszag [11]. It can be outlined as follows.
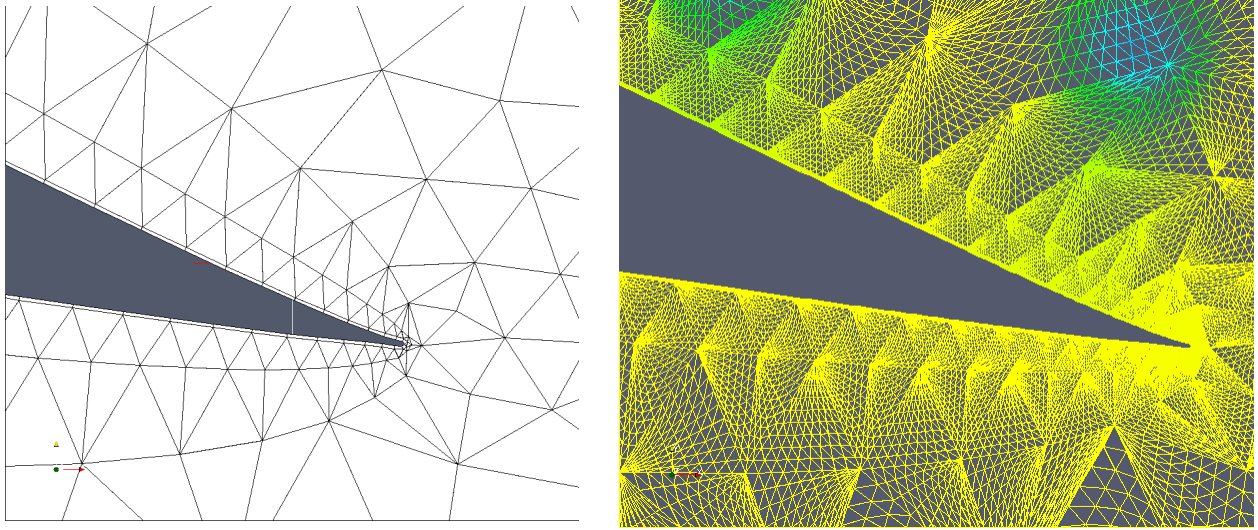
Figure 2: The grid at the tail of the airfoil consisting of a thin quadrilateral layer around the airfoil and triangles around (left).The resolution is increased by additional nodes from the spectral method (right).

(i) Integrate explicitly non-linear term.

$$\frac{\mathbf{u}^* - \mathbf{u}^n}{\Delta t} = \sum_{q=0}^{J-1} \beta_q N(\mathbf{u}^{n-q}),$$ (3)

where $\mathbf{u}^*$ is intermediate velocity, β_q, $(q = 0, ..., J-1)$ are the coefficients of explicit Adams-Bashforth scheme of order J, and γ_q – the coefficients of implicit scheme.

(ii) Solve the Poisson equation for pressure p^{n+1}

$$\nabla^2 p^{n+1} = \nabla \cdot \frac{\mathbf{u}^*}{\Delta t}$$ (4)

with the boundary conditions

$$\frac{\partial p^{n+1}}{\partial \mathbf{n}} = \mathbf{n} \cdot \left[-\sum_{q=0}^{J-1} \beta_q \left(N(\mathbf{u}^{n-q}) \right) - \frac{1}{Re} \sum_{q=0}^{J-1} \beta_q \left(\nabla \times (\nabla \times \mathbf{u}^{n-q}) \right) \right].$$ (5)

(iii) Solve the Helmholz equation for velocity $\mathbf{u}^{n+1}$

$$\frac{\mathbf{u}^{n+1} - \mathbf{u}^*}{\Delta t} = -\nabla p^{n+1} + \sum_{q=0}^{J-1} \gamma_q L(\mathbf{u}^{n+1-q})$$ (6)

The polynomial mode $\varphi_i(\mathbf{x})$ is supported by one element (triangle or quadrilateral) of the mesh, and is explicitly represented in terms of the classical Jacobi polynomials. Although the modes do not form a fully orthogonal basis, they have a good orthogonality property to provide a sparsity of the stiffness and the mass matrices used in the code. The polynomial order for this simulation was set to $p = 9$. Over all the number of degrees of freedom was > 200000 (see fig. 2). In front of the outflow boundary a sponge layer of $2 L_c$ thickness was implemented to dampen unwanted reflection effects[12]. The simulation ran at a time stepping of $dt = 1.25 \cdot 10^{-5}$ and a CFl value of about 0.38 for 20000000 time steps using laminar inflow conditions.
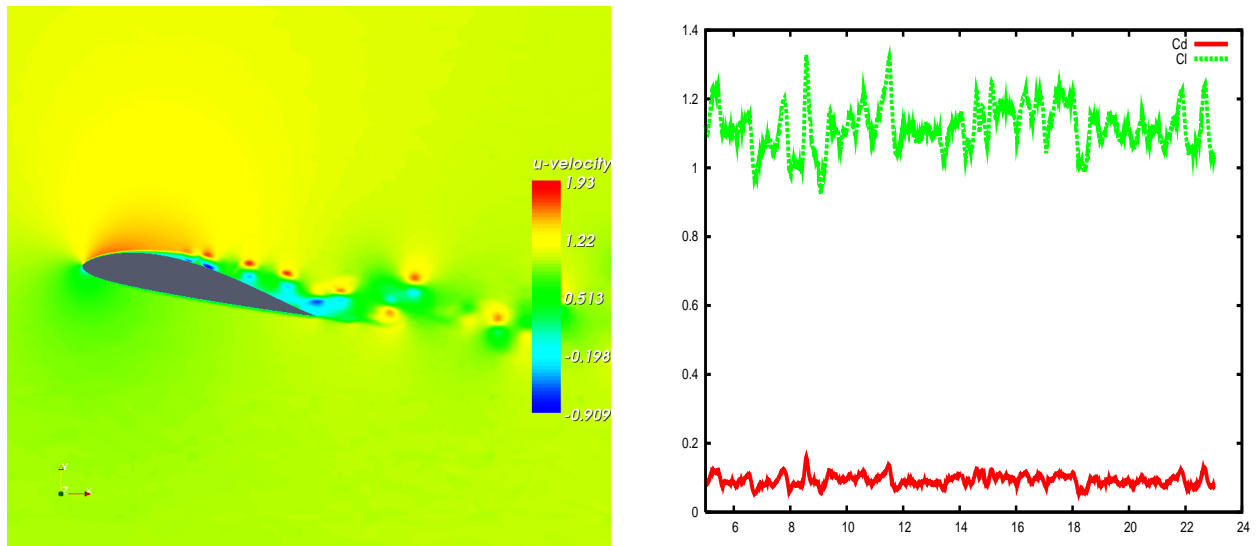
3

Figure 3: The horizontal (u-velocity) flow around the blade, showing a separation after 1/3 of the chord length just after the highest point of the airfoil (left).The time series of lift and drag coefficient on the airfoil, showing fluctuations over the time (right).

3. Results Simulation

In the simulation the flow separates at about 0.3 of the chord length in small Karman street like vortices (fig. 3 (left)). The vortices lead to unsteady forces on the airfoil over the time period (fig. 3 (right)). The average drag is at $\overline{C_d} = 0.09$ fluctuating between a $C_{dmin} = 0.05$ and $C_{dmax} = 0.16$ and the average lift is $\overline{C_l} = 1.12$ with values between $C_{lmin} = 0.92$ and $C_{lmax} = 1.32$.

The frequency of the vortex shedding could be described by a strouhal number of $St = 3.24$. In an unsteady manner the vortices coming from the front of the airfoil also trigger a secondary flow separation at the tail of the airfoil during which a back flow at the tail of the airfoil can be observed.

4. HPIV setup

Holographic particle image velocimetry (HPIV) is a method to investigate 3D flow fields. In HPIV, the position of all the particles present at one instant of time is recorded on a holographic plate (double-exposure). The light scattered from the particle (DEHS, 1 microns diameter (in air)) is made to interfere with the reference laser beam and the interference effect is then recorded locally onto the holographic plate. After the exposed hologram is developed, the particle images can be reconstructed with a reference beam playback system. The images of the backscatter can be reproduced and detected by a CCD camera and thus evaluated for the investigation of the flow field[15][16]. Fig 4 shows the setup of the HPIV measurements at the university of Oldenburg. In the wind tunnel model of the fx79-w151a airfoil with a $L_c = 10cm$ was fixed at an angle of $\alpha = 12°$. In spanwise direction the width of the airfoil was $L_s = 15cm$. The airflow was regulated to a velocity reaching a Reynolds number of $Re = 33333$. The seed density was approximately 110 $particles/mm^3$.

5. HPIV results

There were holograms made from three different regions at the airfoil: One on top right after the tip, one at the tail and one in the wake (see Fig. 5). As they were holograms the resulting pictures were in 3D. The spanwise measuring length was $29.1mm$. To make the results comparable with
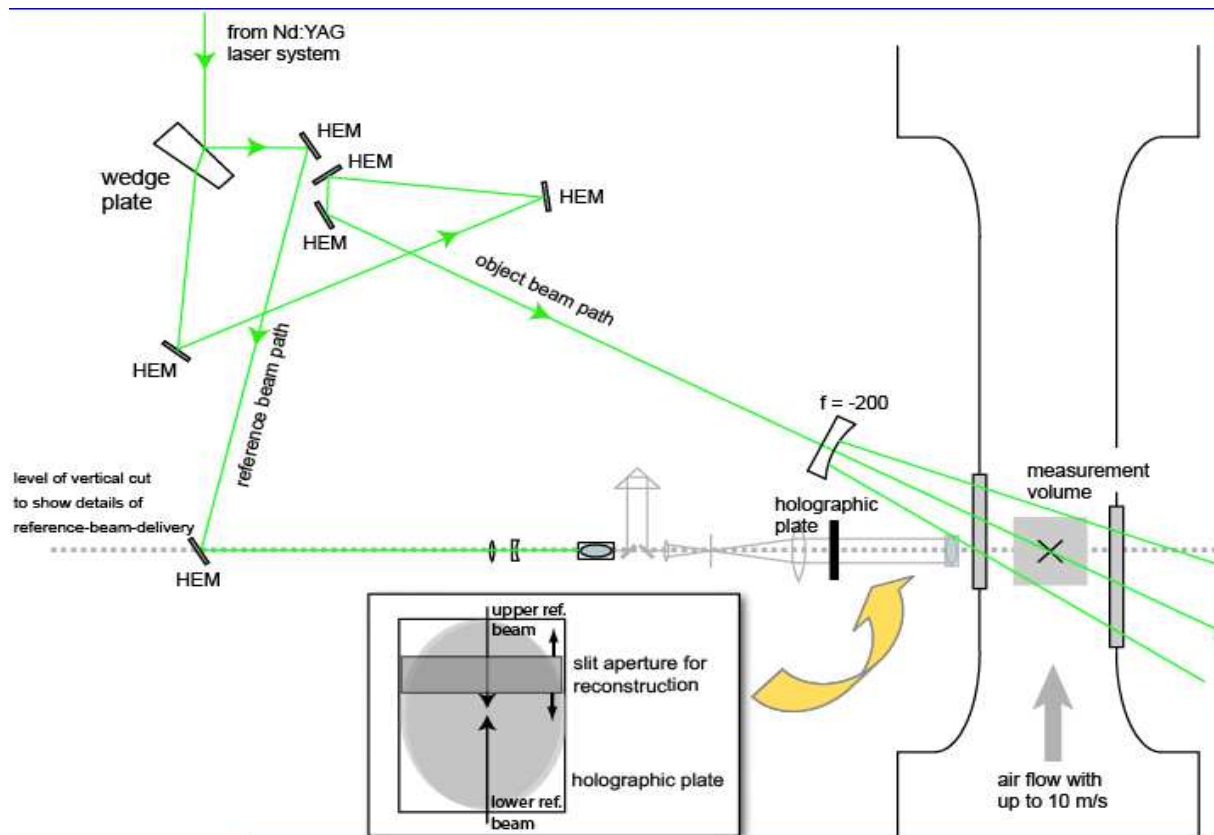
Figure 4: Recording set-up with in-plane reference beams. The illuminated areas on the holographic plate have an almost perfect overlap, a slit aperture can be used for the reconstruction. A single depth position is mapped symmetrically to either side of the holographic plate, depending on whether the according reference beam is incident from left or right. Only for the mid-depth position do both regions on the holographic plate overlap (from [16]).

the 2D simulation the 3D results have been averaged along the spanwise direction and normalized to an inflow velocity of v=1 as in the simulation. The boundaries of the airfoil can be seen in the holograms by a lack of movement. In the tail region there is no information gained from underneath the airfoil due to shading by the airfoil. Also some regions, especially in the front, show some obviously deficient vectors and therefore need to be neglected.

On a qualitative level the measurements and the simulations show some agreements: The separation region of the flow seems to be caught quite well right after the top of the airfoil (see fig.7). Although the HPIV picture shows a lot of distracting deficiant vectors in fig.7 the flow pattern and magnitudes are similar in this region. An increase in flow speed on top of a back flow region can be observed in the tail region of the airfoil within the HPIV image and the simulation. Nevertheless the magnitude of the back flow vorticies seems to be somewhat greater than in the velocimetry image (see fig.8). It is obvious that due to the flow characteristics, some vortices separate from the airfoil and can be detected within the HPIV as well as in the simulation (fig.9). Due to the small section only covered by the HPIV method a real comparison does not seem to be a serious option.

Nevertheless the HPIV pictures do so far give not enough information about the size of the vortices and their separation process. Also some missleading wrongly interpreted vectors, such as inside the area of the airfoil (see. fig.7 or fig.8), made a further evaluation of the HPIV images
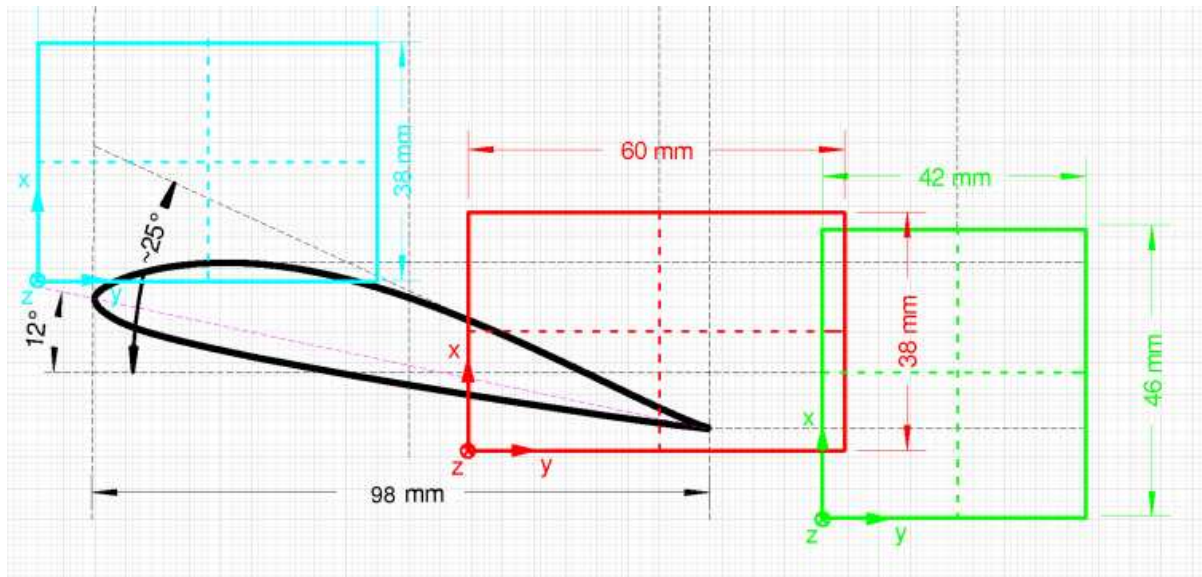
Figure 5: The three regions for the HPIV measurements in the following called front-, tail- and wake-region.
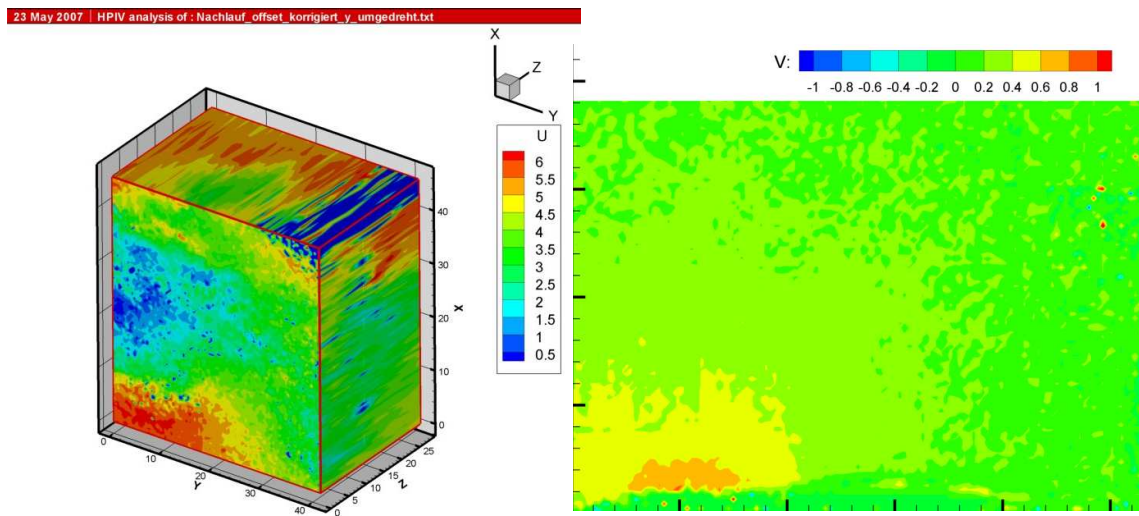

Figure 6: The hologram enables a 3D view of the flow along the airfoil (top left). For the evaluation the spanwise mean is used (mean over z-direction) as can be seen by the v-velocity (perpendicular to the inflow) on the right.

difficult.

6. Conclusions

A 2D simulation using the spectral element code $\mathcal{N}\varepsilon\kappa\mathcal{T}\alpha r$ has been done. At a Reynolds number of $Re = 33000$ a DNS solver has been used. The time resolved simulation shows vortex shedding in the front region of the blade and as a result fluctuations in lift and drag. In the future the same method is to be applied for a 3D simulation as real turbulent separation, which is to be expected at this Reynolds number can only realisticla be observerd in three dimensions.
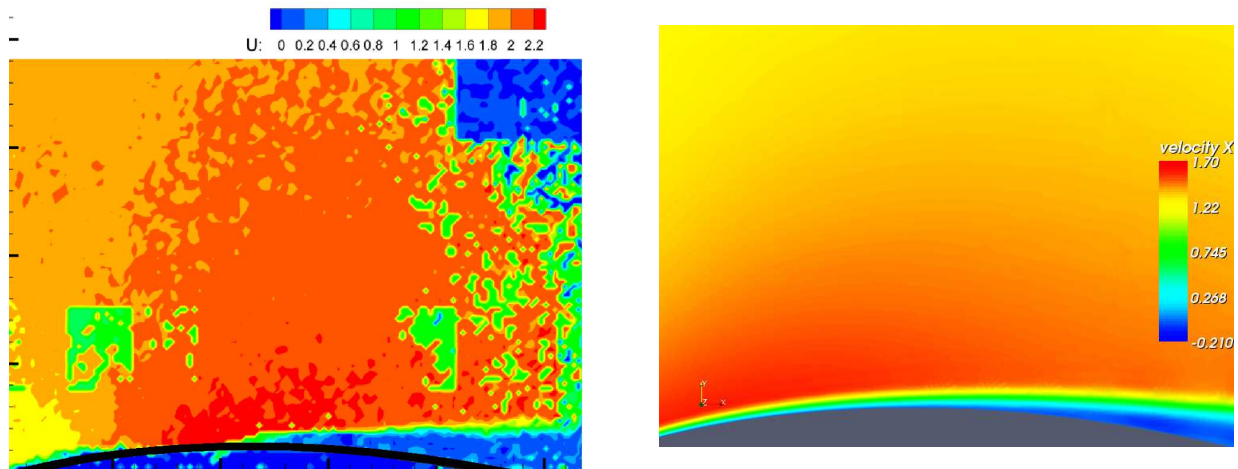
Figure 7: The flow in u direction (left)(inflow direction) shows some areas of vector deficiencies in the hologram. Nevertheless the separation region of the flow can be compared to the one of the simulation. The u-velocity of the simulation in the front-region shown in the bottom right.
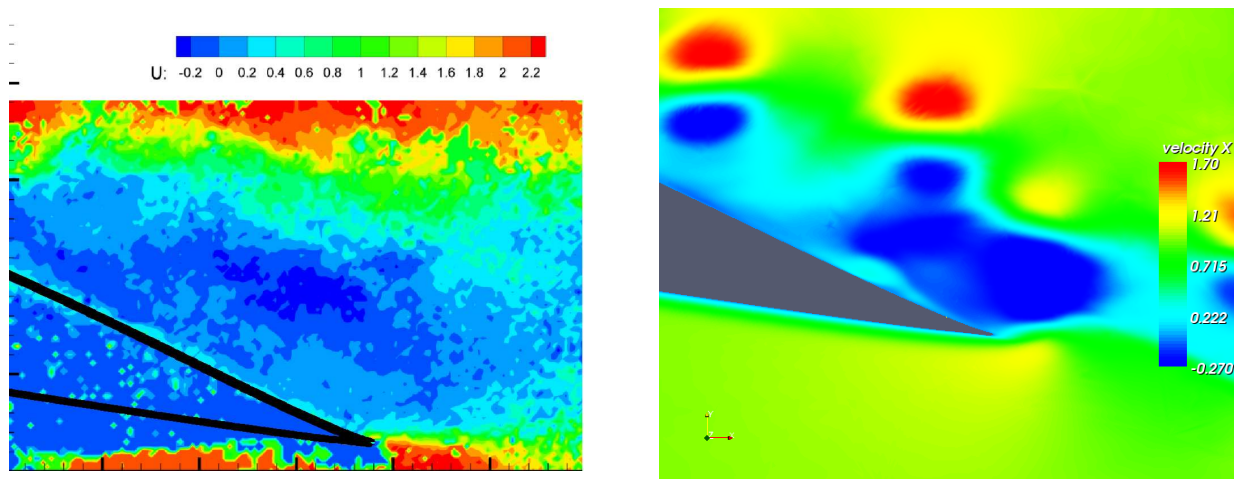

Figure 8: At the tail of the airfoil vortices cause an area of back flow along the airfoil. This can be observed in a larger area at the HPIV measurement (left) than in the simulation (right). The simulation shows more distinct vortex structures.

The results were qualitatively compared to results obtained by HPIV measurements. The HPIV measurements showed also a flow separation in a similar region as the simulation did. The vortices in the back of the airfoil could also be compared. The over all flow magnitudes agreed quite well with the flow patterns of the simulation. Nevertheless the small sections coverd by the HPIV method in the flow made a realistic comparison hard. This and deficient vectors in the measurement prevented a quantitative comparison so far. This, the improvement of the quality of HPIV images and the simulation of a 3D flow will be a task for the future.

References

[1] Schreck S and Robinson M November 2005: Blade Three-Dimensional Dynamic Stall Response to Wind Turbine Operation Condition,*J. of Sol. En. Eng.* **127** pp. 488-495
[2] Larsen J W 2005: Nonlinear Dynamics of Wind Turbine Wings *Ph. D. - Thesis, Aalborg University*
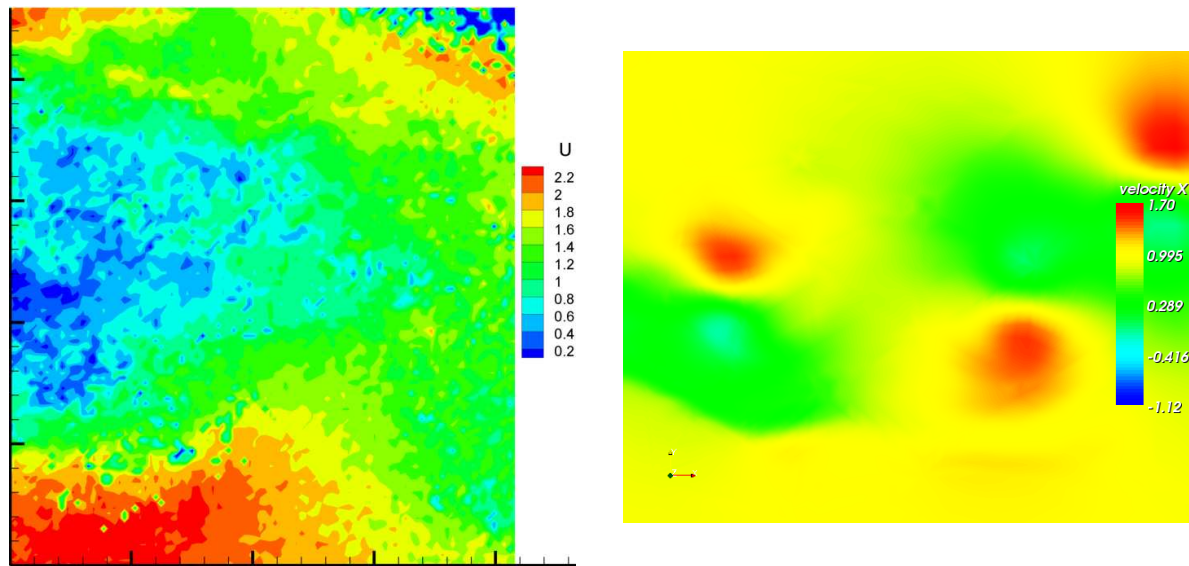
Figure 9: The HPIV measured u-velocity in the wake shows a large vortex structure in the left and maybe some others in the upper part of the upper part of the picture (left). The general structure is caught by the simulation, although the vortex structures of the simulation seem to be smaller (right).

[3] Wagner C 2007: Turbulence modelling and numerical flow simulation of turbulent flows, *Proc. of. EUROMECH Colloquium 464b. Wind Energy Oldenburg, 5.-7.10.2005*

[4] Davidson L, Cokljat D, Fröhlich J, Leschziner M A, Mellen C and Rodi W (Eds.) 2003: LESFOIL - Large Eddy Simulation of Flow Around a High Lift Airfoil, *Notes on Numer. Fluid Mech.* **83** (Springer)

[5] Richez F, Gleize V, Mary I and Basdevant C 2006: Zonal RANS/LES coupling simulation of a transitional and separated flow around an airfoil near stall, *Proc. of Conf. o. Turbulence and Interactions TI2006*, Porquerolles, France

[6] Breuer M and Jovicic N 2001: An LES Investigation of the Seperated Flow Past An Airfoil at High Angle of Attack, *Proc. of the 4th Workshop on DNS and LES Enschede Netherlands*, ERCOFTAC Series **8** (Kluwer Academic Publ., Dordrecht) pp. 165-172

[7] Jovičić N, Breuer M, Jovanović J 2006: Anisotropy–Invariant Mapping of Turbulence in a Flow Past an Unswept Airfoil at High Angle of Attack, *J. Fluids Engineering* **128(3)** pp. 559–567

[8] Terracol M 2005: A zonal RANS/LES approach for airframe trailing-edge noise prediction *Proc. Euromech Col. 467: Turbulent flow and noise generation* Marseille

[9] Bechmann A, Sorensen N N and Johansen J 2007: Atmospheric flow over terrain using hybrid RANS/LES, *Scientific proc. of european wind energy conference* Milan

[10] Karniadakis G E and Sherwin S J 1999 *Spectral/HP Element Methods for CFD* (Oxford: Oxford University Press)

[11] Karniadakis G E, Israeli M and Orszag S A 1991: High-order splitting methods for incompressible Navier-Stokes equations, *J. of Comp. Phys.*, **97**, pp. 414-443

[12] Karniadakis G E and Triantafyllou G E 1992 :Three-dimensional dynamics and transition to turbulence in the wake of bluff objects, *J. Fluid. Mech.* **238,1**

[13] Ma X, Karamanos G S, Karniadakis G E 2000: Dynamics and low-dimensionality of a turbulent near wake, *J. Fluid Mech.*, **410**, pp. 29-65

[14] Williamson C H K 1996: Three-dimensional wake transition, *J. of Fluid Mech.*, **328**, pp. 345-407

[15] Hinsch K D 2002: Holographic particle image velocimetry, *Meas. Sci. Technol.* **13**, pp. R61-R72

[16] Herrmann S F 2006: Optical flow measurements with short coherence holography, *Ph.D - Thesis, Oldenburg University*